Evo-devo dynamics of human brain size

Mauricio González-Forero*[1]

[1]School of Biology, University of St Andrews, Dyers Brae, St Andrews, KY16 9TH, Fife, UK

Abstract

Brain size tripled in the human lineage over four million years, but why this occurred remains uncertain. To advance our understanding of what caused human-brain expansion, we mechanistically replicate it in-silico by modelling the evolutionary and developmental (evo-devo) dynamics of human-brain size. We show that, starting from australopithecine brain and body sizes, the model recovers major patterns of human development and evolution, the evolution of the hominin brain-body allometry, and the evolution of brain and body sizes of six *Homo* species. Analysis reveals that in this model the brain expands because ecology and seemingly culture make brain and developmentally late reproductive tissue sizes socio-genetically covariant. The direction of brain expansion is nearly orthogonal to the direction favoured by unconstrained selection. In contrast to long-held views, in this model, unconstrained selection that does not favour brain expansion provides a force that developmental constraints divert to cause human-brain expansion.

The human brain provides the hardware for stunning achievements, but why it evolved remains unresolved. The fossil record shows a sharp expansion in hominin brain size, tripling over the last four million years from australopithecines to modern humans[1] while some *Homo* were small-brained[2;3]. Many hypotheses exist for why such human brain expansion occurred[4–11]. These hypotheses are actively tested, mostly either with correlative studies[12;13] or comparative studies studying non-hominin species[14;15]. Yet, establishing what were the causes of human brain expansion remains a major multidisciplinary challenge.

Given the practical impossibilities of empirical manipulative testing in humans, a complementary approach to identify the causes of human brain expansion is by means of modelling. Models that can mechanistically replicate the event as much as possible may be analysed to understand what could have caused it. It is of particular interest that such models can make quantitative predictions to understand why a human-sized brain evolved (e.g., of 1.3 kg). Although qualitative predictions are insightful[16–18], they may not be sufficient as what favours a large brain may not necessarily yield a human-sized brain, but possibly one too small or too large for a human.

A recent mathematical model — hereafter, the brain model — can make quantative predictions for brain size evolution[19]. In doing so, the brain model can mechanistically replicate the evolution of adult brain and body sizes of six *Homo* species and much of the timing of human development including the length of childhood, adolescence, and adulthood[20]. Analysis of this brain model[20] has found causal, computational evidence that a challenging ecology[5;11] and seemingly culture[8;10] drove human brain expansion, rather than social interactions as proposed by some influential hypotheses[6;7]. This role of culture is inferred from the model because for human brain expansion to occur in the model it is necessary that an already skilled individual can continue to learn, which cultural knowledge in the population could allow for.

The brain model makes quantitative predictions by explicitly considering development, that is, the construction of the phenotype over life. In particular, the model describes the construction of brain and body sizes over life using energy conservation analysis. To do this, the model follows the approach of West et al.[21], whereby energy conservation analysis yields an equation describing the developmental dynamics of body size depending on parameters measuring metabolic costs that can be easily estimated from data. The brain model implements West et al.'s approach to obtain equations describing the developmental dynamics of brain, reproductive, and somatic tissue sizes depending additionally on genotypic traits controlling energy allocation to the growth of each tissue at each age[19]. The brain model thus depends on parameters measuring brain metabolic costs, which are thought to be a key reason not to evolve large brains[22] and which are easily estimated from existing data[23]. In the brain model, the genotypic traits evolve, which leads to the evolution of brain and body sizes in kg, whose units arise from the empirically estimated metabolic costs.

Further understanding from the brain model has been hindered by the long-standing lack of mathematical synthesis between development and evolution, but this problem has been recently overcome. To consider developmental dynamics, the brain model was evolutionarily static: it had to assume evolutionary equilibrium where fitness is maximised and so was analysed using dynamic optimisation, specifically using optimal control theory[24–26]. This was done because of the long-standing lack of mathematical integration of development and evolution, which meant that there were no tractable methods to mathematically model the evolutionary and developmental dynamics of the brain model. Indeed, approaches available at the time that mathematically integrated developmental and evolutionary dy-

*mgf3@st-andrews.ac.uk

Box 1

How can constraint drive change? At first sight, constraint seen as a barrier would not be able to drive change but only block it. Yet, constraint can be a driver of change as in the following illustration. The Armero tragedy of 1985 involved the death of over 20 thousand people in the Colombian Andes following the eruption of the Nevado del Ruiz volcano. What drove or caused the Armero tragedy? The volcanic eruption melted the snow from the Nevado and the resulting mud travelled a path leading to the town Armero killing nearly all its inhabitants (Box 1 Fig. a; redrawn from ref.[30] p. 21). The mud was constrained to follow that path by the terrain. In this sense, the topographic constraint caused or drove the Armero tragedy by driving the mud to that town rather than to unpopulated areas or to closer and bigger towns such as Manizales. Analogously, developmental constraints limit evolution on the fitness landscape to the path where the relationship between genotype and phenotype holds (Box 1 Fig. b; from ref.[31]). Thus, while selection pushes evolution uphill on the fitness landscape of the genotype and phenotype (or geno-phenotype), developmental constraints drive evolution to an outcome at a path peak.

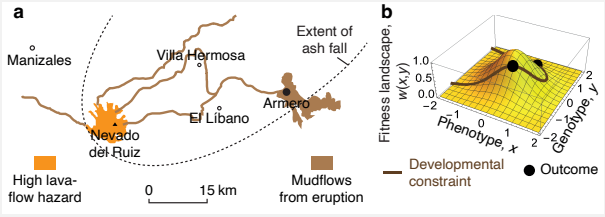

namics required computation of functional derivatives and solution of integro-differential equations[27;28], both of which are prohibitively challenging for the relatively complex brain model. Yet, consideration of the evolutionary dynamics is expected to yield richer insight into why human-sized brains and bodies evolved. In particular, it could allow for analysing how brain developmental constraints translate into genetic covariation, how brain metabolic costs translate into fitness costs, and what selection acts on in the model. This is now possible as the lack of mathematical synthesis between development and evolution has been recently overcome by a tractable mathematical framework that integrates the two, allowing for the simultaneous modeling of the evolutionary and developmental (evo-devo) dynamics in a broad class of models[29].

To gain a deeper understanding of why human brain expansion occurred, here we implement the brain model[20] in the evo-devo dynamics framework[29], which yields the first model of the evo-devo dynamics of human brain size. Our evo-devo dynamics approach mechanistically recovers an exceptionally wide range of observations in the hominin lineage. It also enables detailed analysis revealing that the evolutionary role of ecology and culture in the recovered human brain expansion is not to affect fitness costs or benefits but to generate genetic covariation that drives brain expansion. Moreover, in contrast to long-held views, our analysis reveals that human brain expansion in the model is driven by developmental and consequently socio-genetic constraints rather than selection on brain size (Box 1).

We provide an overview of the model in Methods. We describe the model in detail and derive the necessary equations for the evo-devo analysis in the Supplementary Information (SI). We provide in the SI the computer code written in the freely accessible and computationally fast Julia programming language.

Results

Evo-devo dynamics of brain size

We begin by describing the evo-devo dynamics of human brain size in the model for the scenario that recovers the evolution of *Homo sapiens'* brain and body sizes and other properties of human development — hereafter the eco-social scenario. For simplicity, the model considers only females. The genotype undergoes the following evolutionary dynamics. In our brain evo-devo model, the genotype is described by growth efforts y_{ia} controlling energy allocation to the growth of brain, reproductive, or remaining somatic ($i \in \{\mathrm{b},\mathrm{r},\mathrm{s}\}$) tissues at each age a, where reproductive tissue is defined as referring to preovulatory ovarian follicles. We manually identify evolutionarily initial growth efforts that enable brain expansion under the eco-social scenario previously[20] identified as yielding brain and body sizes of *H. sapiens* scale (blue dots in Fig. 1a-c). This ancestral genotype develops brain and body sizes of australopithecine scale (blue dots in Fig. 1h,o). The genotype asymptotically evolves to the following developmental patterns (red dots in Fig. 1a-c). Effort for brain growth evolves from damped oscillations over ontogeny to slightly more pronounced oscillations (Fig. 1a). Effort for reproductive growth evolves from gradual increase over ontogeny to sharp oscillations trending upwards (Fig. 1b). Effort for somatic growth evolves from gradual decrease over ontogeny to sharp oscillations with three marked peaks (Fig. 1c).

These growth efforts determine the fraction q_{ia} of the growth metabolic rate that is allocated to the growth of tissue i at age a (Fig. 1d-g). The growth metabolic rate is the rate of heat released at rest due to growth. The fraction of growth metabolic rate entails a trade-off in energy allocation, such that energy allocated to the growth of a given tissue at a given age becomes unavailable for the growth of other tissues at that age. Ancestrally, there are two periods at 4-8 and 9-12 years of age with mild energy allocation to brain growth (blue dots in Fig. 1d), which

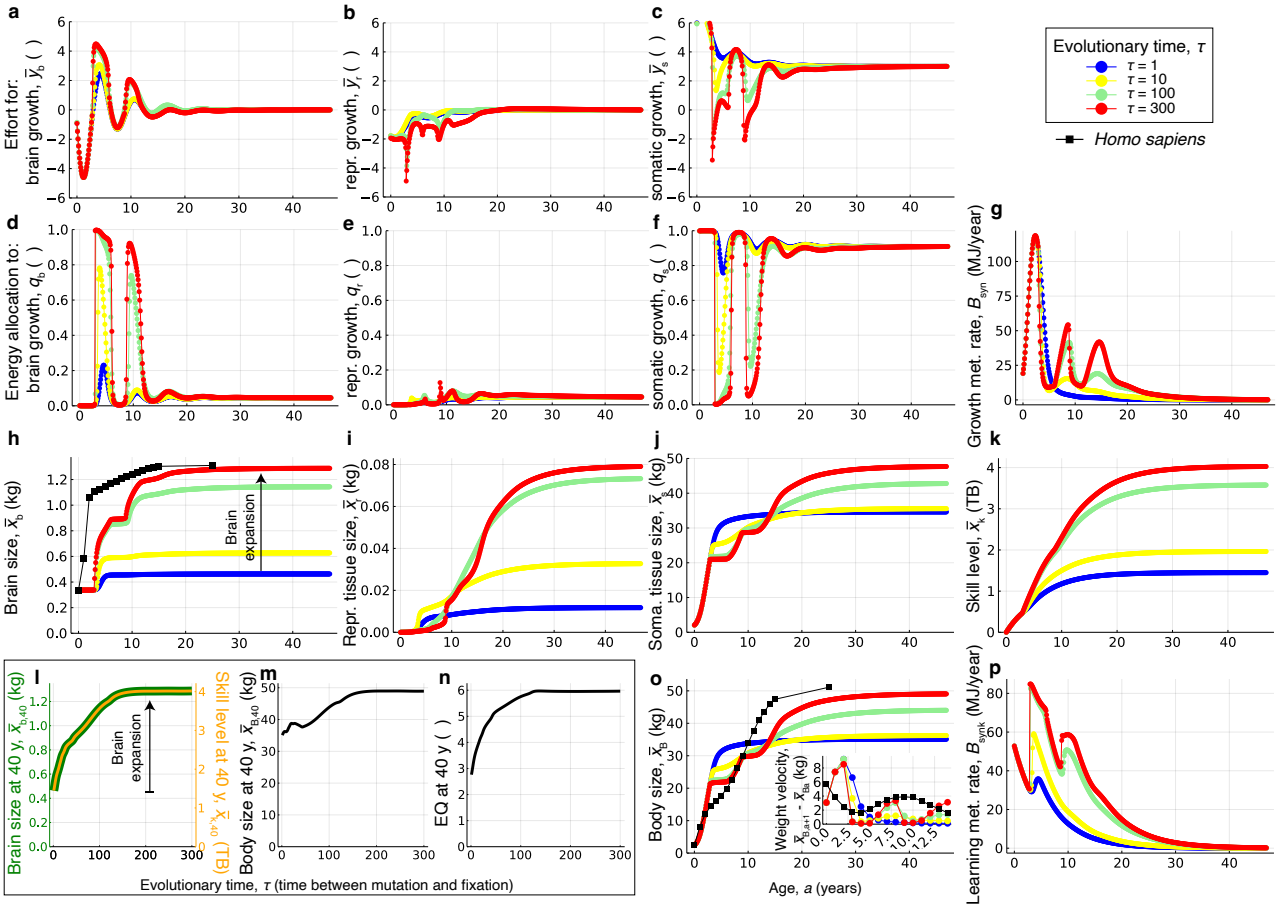

Figure 1: **Evo-devo dynamics of human brain size.** Developmental dynamics are over age (e.g., horizontal axis in **A**) and evolutionary dynamics are over evolutionary time (differently coloured dots; top right label). Evo-devo dynamics of: **a-c,** growth efforts (genotypic traits); **d-f,** energy allocation to growth; **g,** the growth metabolic rate; **h-k,** the phenotypic traits; **o,** body size with inset plotting the yearly weight velocity showing the evolution of two growth spurts; and **p,** the learning metabolic rate. **l-n,** Evolutionary dynamics of brain size, body size, and encephalisation quotient (EQ) at 40 years of age. **h,o,** The mean observed brain and body sizes in a modern human female sample are shown in black squares in **h** and **o** (data from ref.[23] who fitted data from ref.[32]). One evolutionary time unit is the time from mutation to fixation. If gene fixation takes 500 generations and one generation is 22 years, then 300 evolutionary time steps are 3.3 million years. The age bin size is 0.1 year. Halving age bin size (0.05 year) makes the evolutionary dynamics twice as slow but the system converges to virtually the same evolutionary equilibrium (Fig. S1).

correspond to periods of reduced allocation to somatic growth (blue dots in Fig. 1f); in turn, allocation to reproductive growth developmentally increases from zero after 3 years of age and slowly achieves a small maximum value at around 20 years of age (blue dots in Fig. 1e). Over evolution, energy allocation converges to there being two periods at 4-8 and 9-12 years of age with nearly full energy allocation to brain growth (red dots in Fig. 1d), which correspond to periods of nearly absent energy allocation to somatic growth (red dots in Fig. 1f); in turn, allocation to reproductive growth evolves, increasing slightly but remaining small throughout life with various peaks, the most marked occurring at around 9 years of age matching the observed age at menarche[33;34] (red dots in Fig. 1e). The energy allocation to reproductive growth found with the previous optimisation approach[20] was substantial, but this occurred in developmental periods where growth metabolic rate was nearly zero, so such high energy allocation was immaterial.

The obtained evolution of energy allocation to growth yields the following evo-devo dynamics in the phenotype. Adult brain size nearly triples from less than 0.5 kg to around 1.3 kg matching that observed in modern human females[32;35;23] (Fig. 1h). The resulting rate of developmental brain growth in the model is slower than that observed and than that obtained in the previous optimisation approach[20], which was already delayed possibly because the developmental Kleiber's law we use underestimates resting metabolic rate at small body sizes (Fig. C in ref.[19]; Fig. S2B in ref.[36]). The added developmental delay might be partly due to our use of relatively coarse age bins (0.1 year) rather than the (nearly) continuous age used previously[20], although halving age bin size (0.05 year) has no effect (Fig. S1). Another factor possibly contributing to the added developmental delay is that the resulting exact pattern of brain growth depends on the ancestral genotypic traits (compare the red dots of Fig. 1h with those of Fig. S4). These slightly different results from different

ancestral genotypes may be partly because of slow evolutionary convergence to equilibrium, and possibly also because there is socio-genetic covariation only along the path where the developmental constraint is met (Box 1 Fig. b; so $\mathbf{L_z}$ in Eq. M5, a matrix that is a mechanistic, generalised analogue of Lande's[37] **G** matrix, is singular) which means that the evolutionary outcome depends on the evolutionarily initial conditions[38;29].

Reproductive tissue determines fertility in the model, so the developmental onset of reproduction occurs when reproductive tissue becomes appreciably non-zero and gives the age of "menarche" in the model. Reproductive tissue evolves from developmentally early occurrence since around year 4 and small sizes late in life to developmentally late occurrence since around year 9 and large sizes late in life (Fig. 1i). That is, the evolved females have higher fertility and become fertile at a later age relative to ancestral females, consistently with empirical analyses[33;39–41].

As somatic tissue is much larger than brain and reproductive tissues, the evo-devo pattern of body size is similar to that of somatic tissue (Fig. 1j,o). Body size ancestrally grows quickly over development and reaches a small size of around 35 kg (blue dots Fig. 1o), and then evolves so it grows more slowly to a bigger size of around 50 kg (red dots Fig. 1o), consistently with empirical analyses[33;42]. Body size evolves from a smooth developmental pattern with one growth spurt to a kinked pattern with three growth spurts, which are most easily seen as peaks in a weight velocity plot[43;33;44] (Fig. 1o inset).

The three evolved growth spurts qualitatively match the three major growth spurts in modern humans. In human females, the first growth spurt occurs before birth, the second — known as mid-growth spurt — peaks during mid-childhood[45], and the third is the adolescent growth spurt[33;44]. The mid-growth spurt is not observed with the spline fitting method used by Kusawa et al.[23] (black squares in Fig. 1o inset) but it is with kernel fitting used by Gasser et al.[45], which is sometimes preferred[33] (p. 203). Our model thus recovers an ancestral lack of adolescent growth spurt and its evolved presence, which is consistent with previous analyses of fossil and extant primate data[33]. Yet, due to the delayed developmental rate recovered, the growth spurts are ontogenetically delayed in the model relative to observation.

The model offers a mechanistic explanation for the evolution of the mid- and adolescent growth spurts. Previous descriptive mathematical models of human growth replicate growth spurts by being fitted to data[46;47], but their lack of mechanistic underpinng has limited their explanatory ability[33]. The adolescent growth spurt has been suggested to function to end growth[48] at a relatively early age[49] with sexual, psychological, economic, and social implications[33;50]. Tanner[51] introduced a conceptual model to explain the abrupt change during growth spurts, which Bogin[52] later conceptualised in terms of catastrophe theory[33] (p. 208-223). Our model recovers the abrupt change during growth spurts and offers an explanation for their occurrence. In the model, the mid- and adolescent growth spurts are a consequence of brain expansion: they evolve as energy allocation to brain growth evolves from moderate to extreme (Fig. 1d,f), which generates two corresponding peaks in the growth metabolic rate (Fig. 1g) and so a surplus of energy available relative to the energy needed for tissue maintenance during such peaks; the abrupt change during growth spurts arises because of the evolved sudden change in allocation to somatic growth over development (known as a bang-bang strategy in life history and optimal control theories).

The growth spurts we recover depend on the ancestral genotype: for instance, the evolved mid-growth spurt is developmentally sooner thus merging with the first growth spurt if the ancestral genotype is optimal when individuals only face ecological challenges (Fig. S4). In humans, girls experience menarche typically after the adolescent growth spurt, whereas boys usually reach reproductive maturity before the adolescent growth spurt (e.g., ref.[33], Chapter 3). Our evo-devo model finds the reverse to the girl sequence although the correct sequence was found with the previous optimisation approach[20]; perhaps this incorrect sequence of the evo-devo model can be corrected by adjusting the ancestral genotype. Yet, even though the rates of brain and body growth are sensitive to the ancestral genotype, the evolved adult brain and body sizes are much less dependent on such conditions (compare red dots at adult ages in Figs. 1h,o and S4h,o).

Adult skill level evolves expanding from slightly over 1 TB to 4 TB, the units of which arise from the used value of the metabolic cost of memory which is within an empirically informed range[53] (Fig. 1k). The learning metabolic rate, which is the brain's metabolic rate due to learning at each age, increases over evolutionary time (Fig. 1p).

These patterns generate associated expansions in brain, body, and encephalisation quotient (EQ)[54] for 40 year-old individuals (Fig. 1l-n). EQ measures here brain size relative to the expected brain size for a given mammal body size[55]. Adult brain size expands more sharply than adult body size (Fig. 1l,m). Consequently, adult brain size evolves from being ancestrally 3 times larger than expected to be 6 times larger than expected (Fig. 1n). Thus, the brain expands beyond what would be expected from body expansion alone, in which case EQ would remain constant. This observation often suggests that such brain expansion is driven by selection rather than constraint. However, our analyses below reveal otherwise.

Recovery of hominin brain-body allometry

The evolutionary process described above closely recovers the observed brain-body allometry in hominins starting from brain and body sizes of australopithecine scale and generating a slope of 1.86 (Fig. 2a). There is some discrepancy, particularly in adult body size, but some of this discrepancy may arise because the model considers only females whereas the data (green squares) in Fig. 2a are for mixed sexes and allometries may be sex-dependent[56].

To what extent is the recovered brain-body allometry due to selection or constraint? To explore this question, we randomly sampled growth efforts (genotypes) under the eco-social scenario and plotted the developed adult brain and body sizes without evolution, which yields a tight brain-body allometry with slope 0.54 (Fig. 2b). A

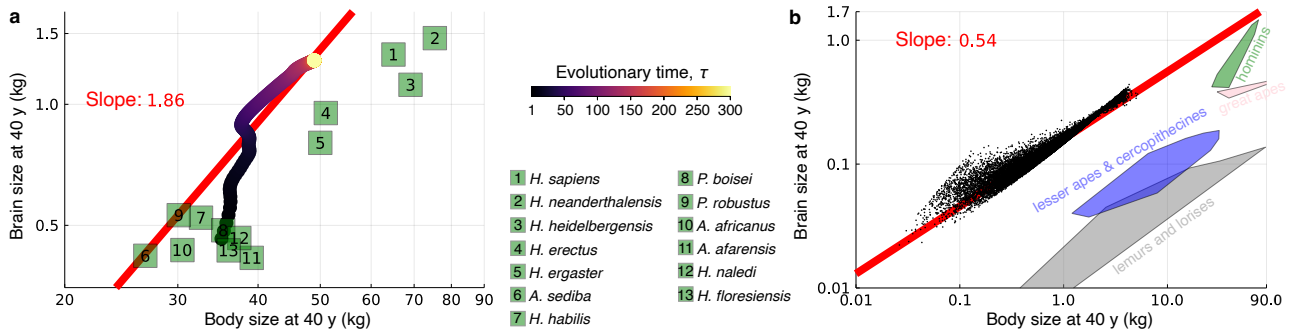

Figure 2: **Recovery of hominin brain-body allometry. a,** Brain size at 40 years of age vs body size at 40 years of age over evolutionary time in log-log scale for the evolutionary process of Fig. 1. A linear regression over this trajectory yields a slope of 1.86 (red line). As test data (i.e., data not fed into the model but to test it against), the values for 12 hominin species are shown in green squares, which excluding *H. floresiensis* and *H. naledi* have a slope of 1.10[57] (from mixed-sex data for 11 species from ref.[57] in turn taken from refs.[58;59], for *H. floresiensis* from ref.[2], and for *H. naledi* from ref.[3]); Pilbeam and Gould[60] found a slope of 1.7 in hominins. *H.*: *Homo*, *A.*: *Australopithecus*, and *P.*: *Paranthropus*. **b,** Dots are brain and body sizes of "non-failed" organisms at 40 years of age developed under the brain model for 10^6 randomly sampled genotypes (i.e., growth efforts, drawn from the normal distribution with mean 0 and standard deviation 4). "Failed" organisms (not shown) at 40 years of age have small bodies (< 100 grams) entirely composed of brain tissue due to tissue decay from birth (Fig. S5). Coloured regions encompass extant and fossil primate species from ref.[57] (excluding three fossil, outlier cercophitecines).

similar slope but with a lower intercept is found in other primates (Fig. 2b;[57]). As there is only development but no evolution, this 0.54 slope arises purely from developmental canalization sensu Waddington[61]. For the sample size used, no organism with random genotype reaches hominin brain and body sizes (green region in Fig. 2b). The recovered high intercept from developmental canalization means that the developed brain size is relatively large for the developed body size; such high intercept arises because of the parameter values in the eco-social scenario including a high proportion of moderately difficult ecological challenges, a weakly decelerating energy extraction efficiency (EEE), and a high metabolic cost of memory (Fig. 6F of ref.[19]). The difference between the 1.86 slope obtained with evolution and the 0.54 slope obtained without it might suggest that the former slope is partly due to selection. However, it is challenging to disentangle selection and constraint in the recovered brain expansion by analysing brain-body allometry, a point made before[62].

Analysis of the action of selection

To draw firmer conclusions regarding what drives the obtained brain expansion, we now quantify genetic covariation and direct (i.e., unconstrained) selection which formally separate the action of constraint and selection on evolution. Such formal separation was first formulated for short-term evolution under the assumption of negligible genetic evolution[37;64] and is now available for long-term evolution under non-negligible genetic evolution[29]. We first analyse the action of selection. In the brain model, fertility is proportional to the size of reproductive tissue whereas survival is constant as a first approximation. Then, in the brain model there is always positive direct selection for ever-increasing size in reproductive tissue, but there is no direct selection for brain size, body size, skill level, or anything else (Fig. 3a-d; Eq. M3). So the fitness landscape in geno-phenotype space (as in Box 1 Fig. b) has no internal peaks and unconstrained selection only favours an ever larger reproductive tissue. Since there is only direct selection for reproductive tissue, the evolutionary dynamics of brain size $\bar{x}_{\mathrm{b}a}$ at age a satisfy

$$\frac{\mathrm{d}\bar{x}_{\mathrm{b}a}}{\mathrm{d}\tau} = \iota \sum_{j=1}^{N_{\mathrm{a}}} L_{x_{\mathrm{b}a},x_{\mathrm{r}j}} \frac{\partial w_j}{\partial x_{\mathrm{r}j}}, \tag{1}$$

where ι is a non-negative scalar measuring mutational input, $L_{x_{\mathrm{b}a},x_{\mathrm{r}j}}$ is the mechanistic additive socio-genetic covariance between brain size at age a and the size of reproductive tissue at age j, w_j is fitness at age j, and $\partial w_j/\partial x_{\mathrm{r}j}$ is the direct selection gradient of reproductive tissue at age j. Eq. (1) shows that brain size evolves in the brain model only because brain size is socio-genetically correlated with reproductive tissue (i.e., setting the socio-genetic covariation between brain and reproductive tissue sizes to zero in Eq. 1, so $L_{x_{\mathrm{b}a},x_{\mathrm{r}j}} = 0$ for all ages a and j, yields no brain size evolution).

Assuming evolutionary equilibrium, the brain model was previously found[20] to recover the evolution of the adult brain and body sizes of six *Homo* species by varying only the proportion of the different types of energy extraction challenges faced at each age and the shape of how EEE relates to skill level. We recover these results with our evo-devo dynamics approach (Fig. 4). The factors identified as driving brain expansion when varying these conditions were an increasing proportion of moderately difficult ecological rather than social challenges and an EEE that switches from decelerating quickly with increasing skill (e.g., a skilled forager cannot further improve their foraging ability) to decelerating slowly (a skilled forager can continue to improve their foraging ability, for instance, by learning from the cultural knowledge "accumu-

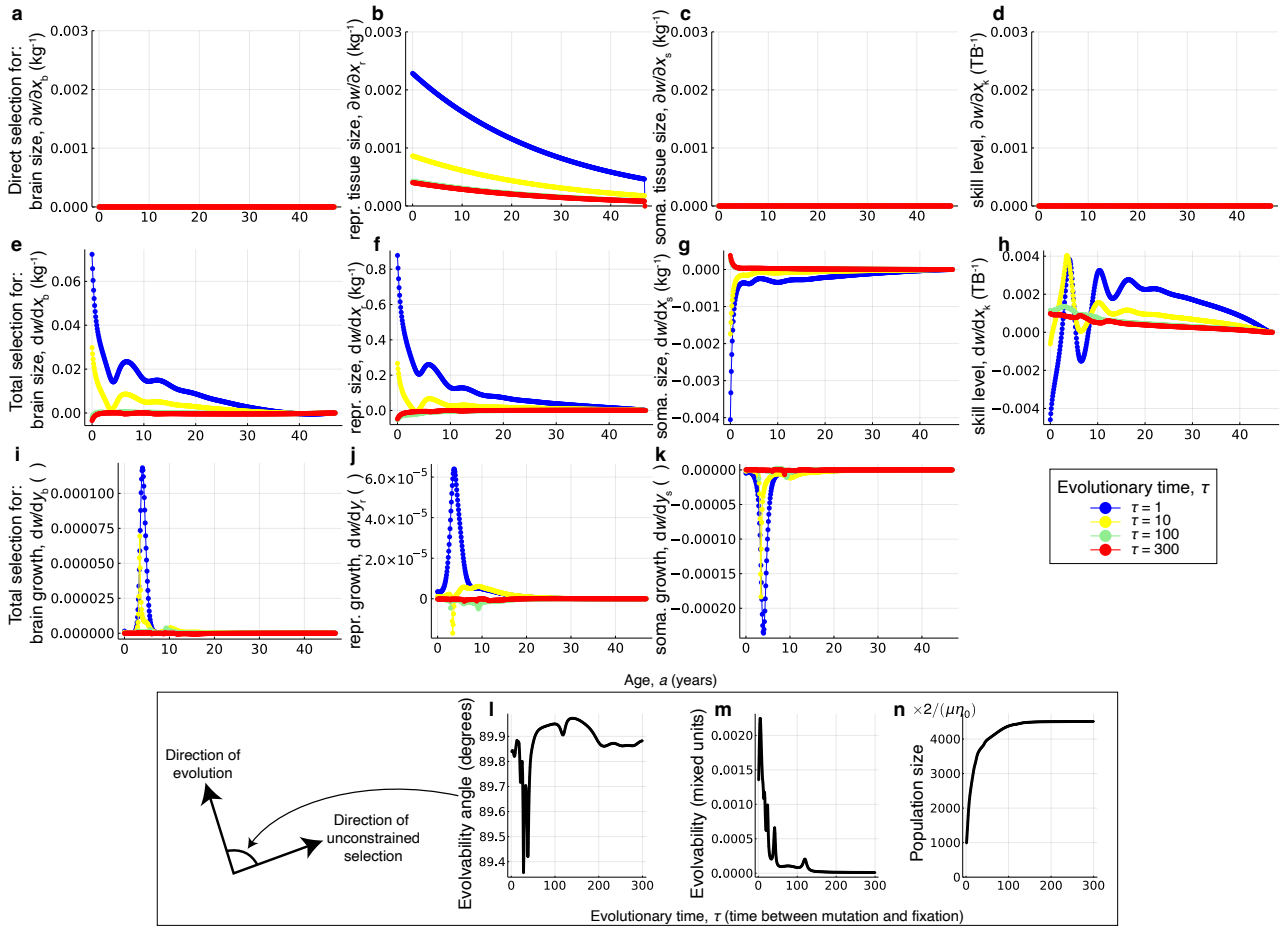

Figure 3: **The action of selection. a-d,** Direct (i.e., unconstrained) selection on brain, reproductive, and somatic tissues, and on skill level at each age over evolutionary time. **e-h,** Total (i.e., constrained) selection on brain, reproductive, and somatic tissues, and on skill level at each age over evolutionary time. **i-k,** Total selection on allocation effort for brain, reproductive, and somatic tissue growth at each age over evolutionary time. **l,** Angle between the direction of evolution and unconstrained selection, both of the geno-phenotype, over evolutionary time. **m,** Evolvability over evolutionary time (0 means no evolvability, 1 means perfect evolvability, SI section S6; Eq. 1 of ref.[63]). **n,** Population size (plot of $\frac{1}{2}\mu\bar{n}^*\eta_0$, so the indicated multiplication yields population size). Mutation rate μ and parameter η_0 can take any value satisfying $0 < \mu \ll 1$ and $0 < \eta_0 \ll 1/(N_g N_a)$, where the number of genotypic traits is $N_g = 3$ and the number of age bins is $N_a = 47\text{y}/0.1\text{y}$. If $\mu = 0.01$ and $\eta_0 = 1/(3 \times 47\text{y}/0.1\text{y})$, then a population size of $1000 \times 2/(\mu\eta_0)$ is 282 million individuals (which is unrealistically large due to our assumption of marginally small mutational variance to facilitate analysis). All plots are for the evolutionary process of Fig. 1.

lated" in the population). This indicated that ecology and culture drive human brain expansion in the model[20].

Our evo-devo dynamics approach enables deeper evolutionary analysis of this finding. In the brain model, challenge proportion and the shape of EEE only directly affect the developmental map ($\mathbf{g}_a$) but not fitness, so varying challenge proportions and the shape of EEE does not affect the direction of unconstrained selection, but only its magnitude (Eqs. S41). Hence, the various evolutionary outcomes matching six *Homo* species[20] (Fig. 4) arise in this model exclusively due to change in developmental constraints and not from change in direct selection on brain size or cognitive abilities. Moreover, from the equation that describes the long-term evolutionary dynamics (Eq. M5) it follows that varying challenge proportions and the shape of EEE only affects evolutionary outcomes (i.e., path peaks; Box 1 Fig. b) by affecting the mechanistic socio-genetic covariation $\mathbf{L}_\mathbf{z}$ (Eq. S32). That socio-genetic covariation determines evolutionary outcomes despite no internal fitness landscape peaks is possible because there is socio-genetic covariation only along the path where the developmental constraint is met (so $\mathbf{L}_\mathbf{z}$ is always singular[29]) and consequently evolutionary outcomes occur at path peaks rather than landscape peaks[31] (Box 1 Fig. b). That is, the various evolutionary outcomes matching six species of *Homo*[20] (Fig. 4) are exclusively due to change in mechanistic socio-genetic covariation described by the $\mathbf{L}_\mathbf{z}$ matrix, by changing the position of path peaks on the peak-invariant fitness landscape. Therefore, ecology and culture drive human brain expansion in the model by affecting developmental and consequently socio-genetic constraints rather than unconstrained selection. Additionally, brain metabolic costs directly affect the developmental map ($\mathbf{g}_a$) and so affect

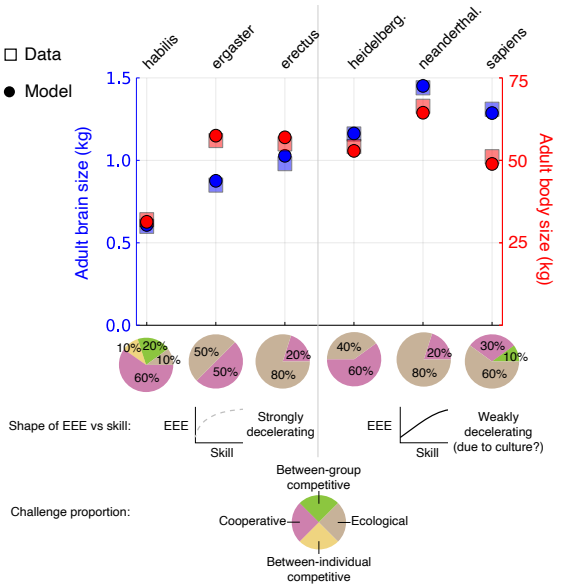

Figure 4: **Evolution of brain and body sizes of six *Homo* species solely by changing socio-genetic covariation.** Adult brain and body sizes six *Homo* species evolve in the model only by changing the challenge proportion and the shape of energy extraction efficiency (EEE) with respect to skill. Squares are the observed brain and body sizes for the corresponding species (data from refs.[23;32;65–69]). Dots are the evolved values in the model for a 40-year-old using our evo-devo dynamics approach under six scenarios starting from the australopithecine ancestral condition (Fig. 1). Pie charts give the challenge proportions used in each scenario. The shape of EEE in each scenario is either strongly (for the left 3 scenarios) or weakly (for the right 3 scenarios) decelerating. These challenge proportions and shape of EEE were identified previously assuming evolutionary equilibrium[20]. In principle, weakly decelerating EEE might arise from culture. Varying challenge proportion and the shape of EEE only varies socio-genetic covariation $\mathbf{L}_{\mathbf{z}}$, but not the direction of the selection gradient $\partial w/\partial \mathbf{z}$ or where it is zero (it never is). The final evolutionary time is 300 for all six scenarios except for the *habilis* scenario, where it is 500 due to slower evolutionary convergence of adult values.

mechanistic socio-genetic covariation ($\mathbf{L}_{\mathbf{z}}$) but do not directly affect fitness (w) and so do not constitute direct fitness costs (Eqs. S8, S10, S2, S9, and M3).

Despite absence of unconstrained selection on brain or skill in the model, there is constrained selection on the various traits. Constrained, or total, selection is measured by total selection gradients that quantify the total effect of a trait on fitness considering the developmental constraints and so how traits affect each other over development[29;70]. Thus, in contrast to direct selection, total selection does not separate the action of selection and constraint. Since we assume there are no absolute mutational constraints (i.e., $\mathbf{H}_{\mathbf{y}}$ is non-singular), evolutionary outcomes occur at path peaks in the fitness landscape where total genotypic selection vanishes ($\mathrm{d}w/\mathrm{d}\mathbf{y} = \mathbf{0}$), which are not necessarily fitness landscape peaks where direct selection vanishes ($\partial w/\partial \mathbf{z} \neq \mathbf{0}$). Constrained selection ancestrally favours increased brain size throughout life (blue circles in Fig. 3e). As evolution advances, constrained selection for brain size decreases and becomes negative early in life, possibly due to our assumption that the brain size of a newborn is fixed and cannot evolve. A similar pattern results for constrained selection on reproductive tissue (Fig. 3f). Somatic tissue is ancestrally totally selected against throughout life, but it eventually becomes totally selected for (Fig. 3g). Constrained selection for skill level ancestrally fluctuates across life but it becomes and remains positive throughout life as evolution proceeds (Fig. 3h). Thus, constrained selection still favours evolutionary change in the phenotype at evolutionary equilibrium, but change is no longer possible (red dots in Fig. 3e-h are at non-zero values). This means that evolution does not and cannot reach the favoured total level of phenotypic change in the model.

Although evolution does not reach the favoured total level of *phenotypic* change in the model, it does reach the favoured total level of *genotypic* change because of our assumption of no absolute mutational constraints. Constrained selection for the genotypic trait of brain growth effort is ancestrally strongly positive around the age of onset of brain growth and evolves toward zero (Fig. 3i). Constrained genotypic selection for reproductive growth effort is ancestrally strongly positive around the age of menarche, transiently evolves to strongly negative around the age of menarche and to positive around the age of a second growth spurt in reproductive tissue, and eventually approaches zero (Fig. 3j). Constrained genotypic selection for somatic growth effort is ancestrally strongly negative around the age of onset of brain growth and evolves toward zero (Fig. 3k). The evolved lack of constrained genotypic selection means that evolution reaches the favoured total level of genotypic change. This also means that evolution stops at a path peak on the fitness landscape (as in Box Fig. b).

The occurrence of total selection for brain size or skill level might suggest that this total selection drives brain expansion in the model, but in this model total selection can change the evolved brain size only due to change in the developmental constraints. This is because total selection equals the product of direct selection and total developmental bias (Eqs. S36 and S37), and in the model changing challenge proportions or the shape of EEE does not affect the direction of direct selection but only affects the direction of total developmental bias by affecting the developmental constraints. Thus, varying total selection can affect evolutionary outcomes in the model only if the developmental constraints are changed.

We can quantify the contribution to brain expansion of the different forms of selection, but this is at the cost of confounding the action of selection and constraint. We first quantify the contributions of direct selection on the various traits. From Eq. (1), the brain expansion in Fig. 1 is 100% due to direct selection on reproductive tissue (i.e., the only non-zero direct selection is on reproductive tissue, so there are no other direct selection gradients contributing). We can alternatively quantify the contributions to brain expansion of total selection on the various *phenotypic* traits. To do this, we note that the evolution-

ary dynamics of brain size $\bar{x}_{\mathrm{b}a}$ equivalently satisfy

$$\frac{\mathrm{d}\bar{x}_{\mathrm{b}a}}{\mathrm{d}\tau} = \iota \sum_{i\in\{\mathrm{b,r,s}\}} \sum_{j=1}^{N_{\mathrm{a}}} L_{x_{\mathrm{b}a},y_{ij}} \sum_{l\in\{\mathrm{b,r,s,k}\}} \sum_{m=1}^{N_{\mathrm{a}}} \frac{\partial x_{lm}}{\partial y_{ij}} \frac{\mathrm{d}w}{\mathrm{d}x_{lm}}, \quad (2)$$

which is in terms of total phenotypic selection ($\mathrm{d}w/\mathrm{d}x_{lm}$). Using this equation, we find that brain expansion in Fig. 1 is, respectively, 14%, 14%, 8%, and 65% due to total selection on brain size, reproductive tissue size, somatic tissue size, and skill level (i.e., these percents are the l-th term in Eq. (2) summed over τ divided by the total over all four l terms; SI section S7 and Fig. S6). Additionally, Eq. (2) can be rearranged to quantify the contributions to brain expansion of total selection on the various *genotypic* traits. Using such rearrangement, we find that brain expansion in Fig. 1 is, respectively, 23%, 10%, and 67% due to total selection on brain growth, reproductive growth, and somatic growth (i.e., these percents are the i-th term in Eq. (2) summed over τ divided by the total over all three i terms). However, these percent contributions confound the action of selection and constraint as they depend on developmental constraints via both total selection and socio-genetic covariation.

Remarkably, throughout human brain expansion in the model, evolution occurs in a maximally diverted direction from that favoured by unconstrained selection. Specifically, evolutionary change in the geno-phenotype is almost orthogonal to unconstrained selection throughout the evolutionary process that yields human brain expansion (Fig. 3l). Evolvability[63], measuring the extent to which evolution proceeds in the direction of unconstrained selection, is ancestrally very small and decreases toward zero as evolution proceeds (Fig. 3m). This means evolution stops because there is no longer socio-genetic variation in the direction of direct selection. The population size quadruples as the brain expands (Fig. 3n), which is broadly consistent with available estimates[71].

Analysis of the action of constraint

To gain further insight into what drives the recovered brain expansion, we now analyse the action of constraint. Since there is only direct selection for reproductive tissue, the equation describing long-term evolution (Eq. M5) entails that whether or not a trait evolves in the model is dictated by whether or not there is (mechanistic) socio-genetic covariation between the trait and reproductive tissue (e.g., Eq. 1).

Examination of such covariation reveals that brain expansion in the model is driven by positive socio-genetic covariation between brain size and developmentally late reproductive tissue. The mechanistic socio-genetic covariation of the various phenotypes with reproductive tissue, and how such covariation evolves, are shown in Fig. 5. Socio-genetic covariation between brain size and reproductive tissue is ancestrally small (Fig. 5a). Shortly later in evolution as brain expansion proceeds, brain size at ages later than around 2 years is negatively socio-genetically covariant with reproductive tissue of until around 10 years, but strongly positively socio-genetically covariant with reproductive tissue of later years (Fig. 5b). This pattern is maintained as evolution proceeds, but the magnitude of covariation decreases and somewhat increases again (Fig. 5c,d). Hence, direct selection on developmentally late reproductive tissue provides a force for reproductive tissue expansion, and socio-genetic covariation diverts this force to cause brain expansion. This occurs even though the force of selection is weaker at advanced ages[72] (i.e., slopes are negative in Fig. 3b), which can be compensated by high socio-genetic covariation with developmentally late reproductive tissue. Such high covariation can arise because of developmental propagation of phenotypic effects of mutations[31]. The role of ecology and culture in driving brain expansion in the brain model is thus to generate positive socio-genetic covariation between brain size and developmentally late reproductive tissue.

The socio-genetic covariation between body size and reproductive tissue, as well as between skill level and reproductive tissue follow a similar pattern (Fig. 5e-l). Hence, the evolutionary expansion in body size and skill level in the model are also caused by their positive socio-genetic covariation with developmentally late reproductive tissue.

The evolution of reproductive tissue size is governed by a different pattern of socio-genetic covariation between reproductive tissue and itself. Ancestrally, the socio-genetic covariance between reproductive tissue and itself increases with age but is relatively small (Fig. 5m). Shortly later in evolution, the socio-genetic covariance of reproductive tissue is higher in magnitude, being strongly positive between developmentally early reproductive tissue as well as between developmentally late reproductive tissue, but strongly negative between developmentally early and late reproductive tissue (Fig. 5n). Hence, in this evolutionary period, developmentally early reproductive tissue evolves smaller sizes because of negative socio-genetic covariation with developmentally late reproductive tissue. In turn, developmentally late reproductive tissue evolves larger sizes because of positive socio-genetic covariation with developmentally late reproductive tissue.

As evolution proceeds, positive socio-genetic covariation in reproductive tissue becomes clustered around the age of menarche (Fig. 5o,p). Hence, reproductive tissue around this age could evolve a larger size from largely direct selection on it but such evolution is prevented by its negative socio-genetic covariation with developmentally later reproductive tissue. Reproductive tissue at ages other than the age of menarche has small or negative socio-genetic covariation with itself. This pattern of clustered socio-genetic covariation does not occur for brain size, body size, or skill level (Fig. S7). In such traits, socio-genetic covariation increases with age and may also increase as evolution proceeds. Such increase in socio-genetic covariation also occurs between brain size and skill level, body size and brain size, and body size and skill level (Fig. S8).

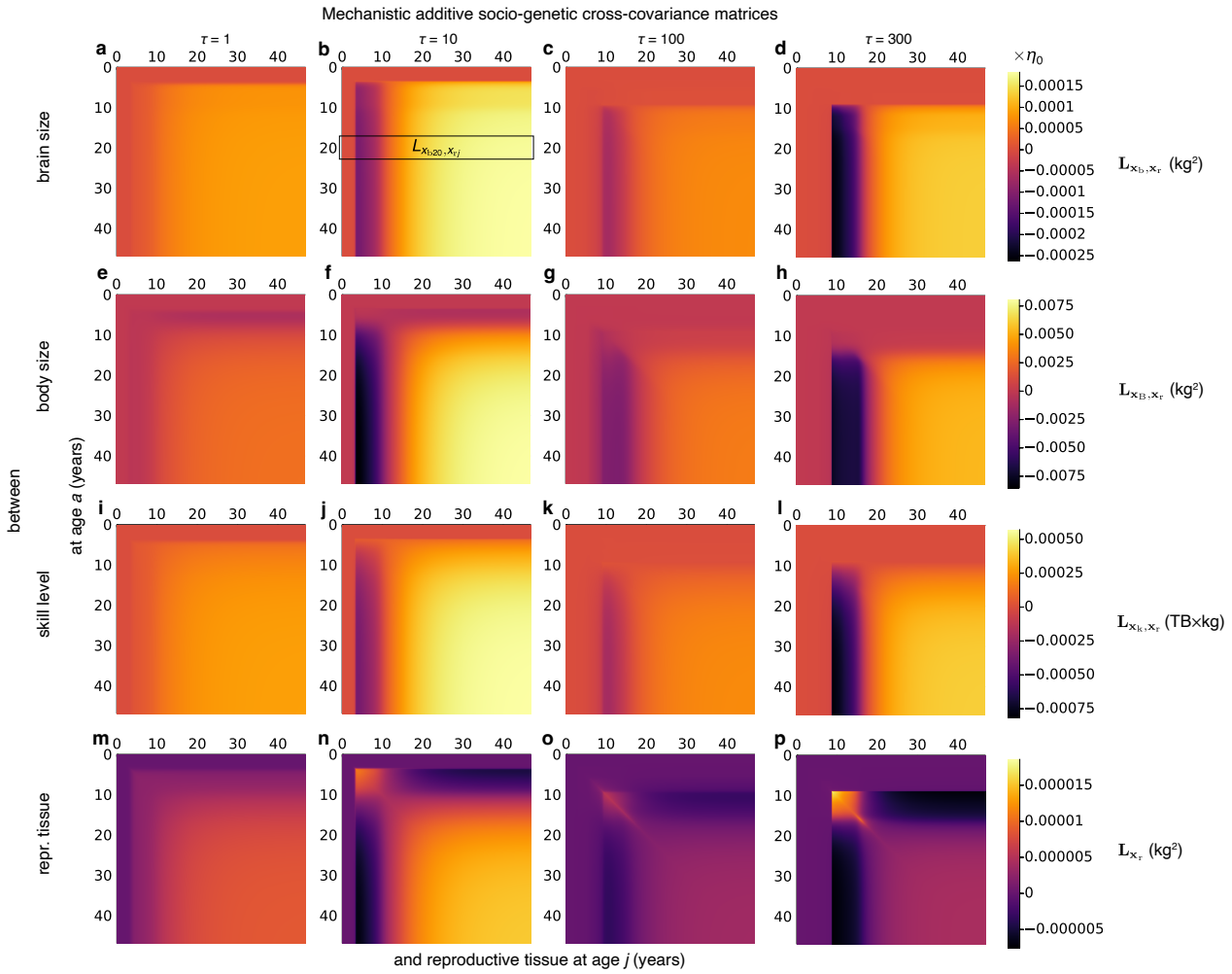

Figure 5: **The action of constraint.** Mechanistic socio-genetic cross-covariance matrix between: **a-d,** brain size (at the ages on vertical axes) and reproductive tissue (at the ages on horizontal axes) over evolutionary time, **e-h,** body size and reproductive tissue, **i-l,** skill level and reproductive tissue, and **m-p,** reproductive tissue and itself. All plots are for the evolutionary process of Fig. 1.

Discussion

We have found that major patterns of human development and evolution can be driven by developmental constraints rather than direct selection. Human brain expansion occurs in this model because brain size is socio-genetically correlated with developmentally late reproductive tissue. Such correlation is created by a moderately challenging ecology and seemingly cumulative culture, which thus drive human brain expansion in this scenario by modulating constraint. This covariation yields an admissible evolutionary path on the fitness landscape (Box 1 Fig. b), a path along which the brain expands, even though the unconstrained direction of steepest increase in fitness does not involve brain expansion. Thus, in this model, human brain expansion is caused by unremarkable selection but particular developmental constraints involving a moderately challenging ecology and seemingly cumulative culture. This constraint-driven brain expansion occurs despite it generating a strongly positive brain-body allometry of 1.86 and a duplication of EQ. While cognitive ability in the form of skill level is not directly under selection in the model, the model can be modified to incorporate such widely considered scenario. Yet, we find that direct selection for cognitive ability is not necessary to recreate a wide range of aspects of human development and evolution, whereas the action of developmental constraints with unexceptional direct selection is sufficient. Change in development without changes in direct selection can thus yield a rich diversity of evolutionary outcomes rather than only evolutionarily transient effects.

These results show that developmental constraints can have major evolutionary roles by driving human brain expansion. Developmental constraints are traditionally seen as preventing evolutionary change[73–75], effectively without ability to generate evolutionary change that is not already favoured by selection. Yet, less prevalent views have highlighted the potential relevance of developmental constraints for human brain evolution (e.g., p. 87 of ref.[76]). Our findings show that while constraints do prevent evolutionary change in some directions, constraints can be "creative"[77] in the sense that they can divert evolutionary change in a direction that causes brain expansion, such that without those constraints brain expansion

is not favoured by selection and does not evolve.

Our results contrast with a previous study finding that direct selection on brain size drove brain expansion in hominins[78]. Such a study used the short-term restricted Lande equation[37;64] for this long-term inference. We use analogous equations that describe long-term evolution and that additionally formally separate the evolutionary effects of developmental constraints and direct selection — a separation that has otherwise not been clear-cut[79]. By doing so, we have found that human brain expansion and various features of human development could have been driven by developmental constraints and that the directional nature of human brain expansion should not be interpreted as necessarily being driven by selection.

Although brain expansion is driven by constraint in the model analysed, such brain expansion is not easily understood as a consequence of body expansion. Brain-body allometry may suggest that brain expansion could result from constraint as a result of body expansion[75;12]. We find that the recovered brain-body allometry is an emergent property that developmentally depends on complex gene-gene and gene-phenotype interactions and evolutionarily depends on mechanistic socio-genetic covariation. In the model, there is no direct selection for body size, so unconstrained selection on body size does not drive brain expansion. Brain and body sizes expand in the model because each is socio-genetically correlated with reproductive tissue, which is the only trait directly selected in the model.

The model provides insight into further debated questions. Variation in the timing of brain development at molecular, cellular, and histological levels has been proposed to lead to evolution of brain diversity[80–82]. Our results are consistent with these views. Adaptive explanations for the protracted human childhood have been advanced (e.g., ref.[83] as discussed on p. 82 of ref.[33], and ref.[84]). In the model, a protracted human childhood arises from the trade-off of energy allocation between brain and somatic growth, so it is a consequence of brain expansion rather than being selected for. Mosaic evolution, whereby different parts of the brain or the body evolve separately, is often taken as evidence against evolutionary constraints (e.g., end of section 2b of ref.[75]). This is not supported by the model as we find that constraints can be drivers of brain expansion despite mosaic evolution as brain and body sizes evolve differently in the model. Brain metabolic costs are widely seen as a key factor preventing brain expansion[22;85;23]. We find that such costs are not fitness costs in the model, but instead affect mechanistic socio-genetic covariation and so the admissible path on the fitness landscape, thus modulating path peaks and evolutionary outcomes. The formulas provided by the evo-devo dynamics framework allow one to compute how brain metabolic costs are transformed into mechanistic socio-genetic covariation or into fitness costs.

Our evo-devo dynamics approach offers a powerful method to advance brain evolution research. A run of the brain model using dynamic optimisation took approximately 3 days to complete[20], whereas using our evo-devo dynamics approach it takes approximately 3 minutes. This computational speed opens the door to implement powerful methods of simulation-based inference[86] that have been very successful in other fields, such as in the discovery of the Higgs boson or in establishing that humans are causing climate change, but remain underexploited in human brain evolution research.

Methods

Model overview. The evo-devo dynamics framework we use[29] is based on adaptive dynamics assumptions[87;88]. The framework considers a resident, well-mixed, finite population with deterministic population dynamics where individuals can be of different ages and reproduction is clonal. Population dynamics occur in a fast ecological timescale and evolutionary dynamics occur in a slow evolutionary timescale. Individuals have genotypic traits, collectively called the genotype, that are directly specified by genes (e.g., a continuous representation of nucleotide sequence, or traits assumed to be under direct genetic control). Also, individuals have phenotypic traits, collectively called the phenotype, that are developed, that is, constructed over life. A function $\mathbf{g}_a$, called the developmental map, describes how the phenotype is constructed over life and gives the developmental constraint. The developmental map can be non-linear, evolve, change over development, and take any differentiable form with respect to its arguments. Mutant individuals of age a have fertility f_a (rate of offspring production) and survive to the next age with probability p_a. The evo-devo dynamics framework provides equations describing the evolutionary dynamics of genotypic and phenotypic traits in gradient form, thus describing long-term genotypic and phenotypic evolution as the climbing of a fitness landscape while guaranteeing that the developmental constraint is met at all times.

The brain model[19;20] provides a specific developmental map $\mathbf{g}_a$, fertility f_a, and survival p_a, which can be fed into the evo-devo dynamics framework to model the evolutionary dynamics of the developed traits studied. More specifically, the brain model considers a female population, where each individual at each age has three tissue types — brain, reproductive, and remaining somatic tissues — and a skill level. Reproductive tissue is defined as referring to pre-ovulatory ovarian follicles, so that reproductive tissue is not involved in offspring maintenance, which allows for writing fertility as being proportional to the mass of reproductive tissue, in accordance with observation[89]. As a first approximation, the brain model lets the survival probability at each age be constant. At each age, each individual has an energy budget per unit time, her resting metabolic rate B_{rest}, that she uses to grow and maintain her tissues. The part of this energy budget used in growing her tissues is her growth metabolic rate B_{syn}. A fraction of the energy consumed by the reproductive tissue is for producing offspring, whereas a fraction of the energy consumed by the brain is for gaining (learning) and maintaining (memory) skills. Each individual's skill level emerges from this energy bookkeeping rather than it being assumed as given by brain size. Somatic tis-

sue does not have a specific function but it affects body size, thus affecting the energy budget because of Kleiber's law[90] which relates resting metabolic rate to body size by a power law. Genes control the individual's energy allocation effort into growing brain, reproductive, and somatic tissues at each age. The individual obtains energy by using her skills to overcome energy-extraction challenges that can be of four types: ecological (e.g., foraging alone), cooperative (e.g., foraging with a peer), between-individual competitive (e.g., scrounging from a peer), and between-group competitive (e.g., scrounging with a peer from two peers). The probability of facing a challenge of type j at a given age is P_j ($\sum_{j=1}^{4} P_j = 1$, where $j \in \{1,\dots,4\}$ indexes the respective challenge types).

We describe the brain model with the notation of the evo-devo dynamics framework as follows. The model considers four phenotypic traits (i.e., $N_\mathrm{p} = 4$): the mass of brain, reproductive, and somatic tissues, and the skill level at each age. For a mutant individual, the brain size at age $a \in \{1,\dots,N_\mathrm{a}\}$ is $x_{\mathrm{b}a}$ (in kg), the size of reproductive tissue at age a is $x_{\mathrm{r}a}$ (in kg), the size of the remaining somatic tissue at age a is $x_{\mathrm{s}a}$ (in kg), and the skill level at age a is $x_{\mathrm{k}a}$ (in terabytes, TB). The units of phenotypic traits (kg and TB) arise from the units of the parameters measuring the unit-specific metabolic costs of maintenance and growth of the respective trait. The vector $\mathbf{x}_a = (x_{\mathrm{b}a}, x_{\mathrm{r}a}, x_{\mathrm{s}a}, x_{\mathrm{k}a})^\intercal$ is the mutant phenotype at age a. Additionally, the model considers three genotypic traits (i.e., $N_\mathrm{g} = 3$): the effort to grow brain, reproductive, and somatic tissues at each age. For a mutant individual, the growth effort at age a for brain is $y_{\mathrm{b}a}$, for reproductive tissue is $y_{\mathrm{r}a}$, and for the remaining somatic tissue is $y_{\mathrm{s}a}$. These growth efforts are dimensionless and can be positive or negative, so they can be seen as measured as the difference from a baseline growth effort. The vector $\mathbf{y}_a = (y_{\mathrm{b}a}, y_{\mathrm{r}a}, y_{\mathrm{s}a})^\intercal$ is the mutant growth effort at age a, which describes the mutant genotypic traits at that age. The growth efforts generate the fraction $q_{ia}(\mathbf{y}_a)$ of the growth metabolic rate B_syn allocated to growth of tissue $i \in \{\mathrm{b},\mathrm{r},\mathrm{s}\}$ at age a (q_{ia} corresponds to the control variables u in refs.[19;20]). To describe the evolutionary dynamics of the phenotype as the climbing of a fitness landscape, the evo-devo dynamics framework defines the mutant geno-phenotype at age a as the vector $\mathbf{z}_a = (\mathbf{x}_a;\mathbf{y}_a)$ (the semicolon indicates a linebreak). The mutant phenotype across ages is $\mathbf{x} = (\mathbf{x}_1;\dots;\mathbf{x}_{N_\mathrm{a}})$, and similarly for the other variables. The mutant's i-th phenotype across ages is $\mathbf{x}_{i\bullet} = (x_{i1},\dots,x_{iN_\mathrm{a}})^\intercal$ for $i \in \{\mathrm{b},\mathrm{r},\mathrm{s},\mathrm{k}\}$. The mutant's i-th genotypic trait across ages is $\mathbf{y}_{i\bullet} = (y_{i1},\dots,y_{iN_\mathrm{a}})^\intercal$ for $i \in \{\mathrm{b},\mathrm{r},\mathrm{s}\}$. The resident traits are analogously denoted with an overbar (e.g., $\bar{\mathbf{x}}$).

The brain model describes development by providing equations describing the developmental dynamics of the phenotype. That is, the mutant phenotype at age $a+1$ is given by the developmental constraint

$$\mathbf{x}_{a+1} = \mathbf{g}_a(\mathbf{x}_a, \mathbf{y}_a, \bar{x}_{\mathrm{k}a}). \tag{M1}$$

The equations for the developmental map $\mathbf{g}_a$ are given in the SI and were previously derived from mechanistic considerations of energy conservation following the reasoning of West et al.'s metabolic model of ontogenetic growth[21] and phenomenological considerations of how skill relates to energy extraction[19;20]. The developmental map of the brain model depends on the skill level of social partners of the same age (i.e., peers), $\bar{x}_{\mathrm{k}a}$, because of social challenges of energy extraction (where $P_1 < 1$) so we say that development is social. When individuals face only ecological challenges (i.e., $P_1 = 1$), development is not social.

The evo-devo dynamics are described by the developmental dynamics of the phenotypic traits given by Eq. (M1) and by the evolutionary dynamics of the genotypic traits. The latter are given by the canonical equation of adaptive dynamics[87]

$$\frac{\Delta\bar{\mathbf{y}}}{\Delta\tau} = \iota \mathbf{H}_\mathbf{y} \frac{\mathrm{d}w}{\mathrm{d}\mathbf{y}}, \tag{M2}$$

where τ is evolutionary time, ι is a non-negative scalar measuring mutational input and is proportional to the mutation rate and carrying capacity, and $\mathbf{H}_\mathbf{y} = \mathrm{cov}[\mathbf{y},\mathbf{y}]$ is the mutational covariance matrix (H for heredity; derivatives are evaluated at resident trait values throughout and we use matrix calculus notation as in Eq. S1). Due to age-structure, a mutant's relative fitness is $w = \sum_{a=1}^{N_\mathrm{a}} w_a = \frac{1}{T}\sum_{a=1}^{N_\mathrm{a}} (\phi_a f_a + \pi_a p_a)$, where f_a and p_a are a mutant's fertility and survival probability at age a, T is generation time, and ϕ_a and π_a are the forces[72] of selection on fertility and survival at that age (T, ϕ_a, and π_a are functions of the resident but not mutant trait values). After substitution and simplification, a mutant's relative fitness reduces to

$$w = \frac{1}{\sum_{a=1}^{N_\mathrm{a}} a p^{a-1} \bar{x}_{\mathrm{r}a}} \sum_{j=1}^{N_\mathrm{a}} \left(p^{j-1} x_{\mathrm{r}j} + \sum_{k=j+1}^{N_\mathrm{a}} p^{k-1} \bar{x}_{\mathrm{r}k} \right), \tag{M3}$$

where p is the constant probability of surviving from one age to the next. This fitness function depends directly on the mutant's reproductive tissue size, but only indirectly on metabolic costs via the developmental constraint (i.e., after substituting $x_{\mathrm{r}j}$ for the corresponding entry of Eq. (M1)).

Eq. (M2) thus depends on the total selection gradient of genotypic traits $\mathrm{d}w/\mathrm{d}\mathbf{y}$, which measures total genotypic selection. While Lande's[37] selection gradient measures unconstrained selection by using partial derivatives (∂), total selection gradients measure constrained selection by using total derivatives (d). Lande's selection gradient thus measures the direction in which selection favours evolution to proceed without considering any constraint, whereas total selection gradients measure the direction in which selection favours evolution considering the developmental constraint (M1). The total selection gradient of genotypic traits for the brain model is

$$\frac{\mathrm{d}w}{\mathrm{d}\mathbf{y}} = \frac{\partial \mathbf{x}^\intercal}{\partial \mathbf{y}} \frac{\mathrm{d}w}{\mathrm{d}\mathbf{x}} = \frac{\mathrm{d}\mathbf{x}^\intercal}{\mathrm{d}\mathbf{y}} \frac{\partial w}{\partial \mathbf{x}}. \tag{M4}$$

Eq. (M4) shows that total genotypic selection can be written in terms of either total phenotypic selection ($\mathrm{d}w/\mathrm{d}\mathbf{x}$) or direct phenotypic selection ($\partial w/\partial \mathbf{x}$). Eqs. (M1) and (M2) together describe the evo-devo dynamics. Eq. (M2) entails that total genotypic selection vanishes at evolutionary equilibria if there are no absolute mutational constraints (i.e., if $\iota > 0$ and $\mathbf{H}_\mathbf{y}$ is non-singular). Moreover,

since there are more phenotypic traits than genotypic traits ($N_p > N_g$), the matrices $\partial \mathbf{x}^\intercal/\partial \mathbf{y}$ and $\mathrm{d}\mathbf{x}^\intercal/\mathrm{d}\mathbf{y}$ have fewer rows than columns and so are singular; hence, setting Eq. (M4) to zero implies that evolutionary equilibria can occur with persistent direct and total phenotypic selection in the brain model.

While we use Eqs. (M1) and (M2) to compute the evo-devo dynamics, those equations do not describe phenotypic evolution as the climbing of an adaptive topography. To analyse phenotypic evolution as the climbing of an adaptive topography, we use the following. The evo-devo dynamics framework[29] shows that long-term phenotypic evolution can be understood as the climbing of a fitness landscape by simultaneously following genotypic and phenotypic evolution, which for the brain model is given by

$$\frac{\mathrm{d}\bar{\mathbf{z}}}{\mathrm{d}\tau} = \iota \mathbf{L}_\mathbf{z} \frac{\partial w}{\partial \mathbf{z}}, \tag{M5}$$

since $\mathbf{z} = (\mathbf{x};\mathbf{y})$ includes the phenotype $\mathbf{x}$ and genotypic traits $\mathbf{y}$. The vector $\partial w/\partial \mathbf{z}$ is the direct selection gradient of the geno-phenotype, measuring unconstrained selection on the phenotype and genotypic traits (as in Lande's[37] selection gradient). The matrix $\mathbf{L}_\mathbf{z}$ is the mechanistic additive socio-genetic cross-covariance matrix of the geno-phenotype, for which the evo-devo dynamics framework provides formulas that guarantee that the developmental constraint (M1) is met at all times (L for legacy). The matrix $\mathbf{L}_\mathbf{z}$ is asymmetric due to social development; if individuals face only ecological challenges, development is not social and $\mathbf{L}_\mathbf{z}$ reduces to $\mathbf{H}_\mathbf{z}$, the mechanistic additive genetic covariance matrix of the geno-phenotype, which is symmetric ($\mathbf{H}_\mathbf{x}$ is a mechanistic version of Lande's[37] $\mathbf{G}$ matrix: whereas $\mathbf{H}_\mathbf{x}$ involves total derivatives describing the total effect of genotype on phenotype, $\mathbf{G}$ is defined in terms of regression of phenotype on genotype; hence, $\mathbf{H}_\mathbf{x}$ and $\mathbf{G}$ have different properties including that mechanistic heritability can be greater than one). The matrix $\mathbf{L}_\mathbf{z}$ is always singular because it considers both the phenotype and genotypic traits, so selection and development jointly define the evolutionary outcomes even with a single fitness peak[31]. Eq. (M5) and the formulas for $\mathbf{L}_\mathbf{z}$ entail that evolution proceeds as the climbing of the fitness landscape in geno-phenotype space, where the developmental constraint (M1) provides the admissible evolutionary path, such that evolutionary outcomes occur at path peaks rather than landscape peaks if there are no absolute mutational constraints[31].

We implement the developmental map of the brain model into the evo-devo dynamics framework to study the evolutionary dynamics of the resident phenotype $\bar{\mathbf{x}}$, including the resident brain size $\bar{\mathbf{x}}_{\mathrm{b}\bullet}$.

Six *Homo* scenarios. It was previously found[20] that, at evolutionary equilibrium, the brain model recovers the evolution of the adult brain and body sizes of six *Homo* species. These six scenarios are given in Fig. 4. The scenarios yielding brain and body sizes of *H. sapiens*, *neardenthalensis*, and *heidelbergensis* scale use a weakly decelerating EEE: specifically, these scenarios use exponential competence with parameter values given in Regime 1 of Table S1and with submultiplicative cooperation (Eq. S5). We call eco-social the scenario yielding brain and body sizes of *H. sapiens* scale; we call ecological the same scenario but setting the proportion of ecological challenges to one ($P_1 = 1$). In turn, the scenarios yielding brain and body sizes of *erectus*, *ergaster*, and *habilis* scale use a strongly decelerating EEE: specifically, these scenarios use power competence with parameter values given in Regime 2 of Table S1and with additive cooperation (Eq. S5). In the main text, we describe the evo-devo dynamics under the eco-social scenario that was previously found[20] to yield *H. sapiens*-sized brains and bodies. For illustration, in the SI we also give the evo-devo dynamics of the ecological scenario (Fig. S3).

Ancestral genotypic traits. To solve the evo-devo dynamics, we must specify the ancestral resident genotypic traits giving the resident growth efforts $\bar{\mathbf{y}}$ at the initial evolutionary time. We find that the outcome depends on such ancestral conditions: for instance, there is bistability in brain size evolution, so there are at least two path peaks on the fitness landscape as follows. Using somewhat "naive" ancestral growth efforts (SI section S4) in the eco-social scenario yields an evolutionary outcome with no brain, where residents have a somewhat semelparous life-history reproducing for a short period early in life followed by body shrinkage (Fig. S2). In contrast, using highly specified ancestral growth efforts in the eco-social scenario yields adult brain and body sizes of *H. sapiens* scale (Fig. 1). This bistability does not arise under the ecological scenario which yields brain expansion under the same somewhat naive ancestral growth efforts (Fig. S3). Thus, for the the eco-social scenario to yield brain and body sizes of *H. sapiens* scale it requires ancestral conditions that already yield large brains, either with the highly specified conditions developmentally yielding australopithecine brain and body sizes (Fig. 1) or with the ecologically optimal growth efforts that developmentally yield brain and body sizes approaching those of Neanderthals (Fig. S4). In the main text, we present the results for the eco-social scenario with the highly specified ancestral conditions. This may be biologically interpreted as a requirement to evolve from ancestors that already had a genotype yielding some ontogenetic brain growth while having large brains at birth.

Acknowledgments

I thank A. Gardner, K. Laland, and R. Patchett for comments on previous versions of the manuscript. I thank A. Gardner for funding and S.D. Healy and C. Rutz for discussion. A. Gardner suggested to randomly sample genotypic traits to evaluate the resulting brain-body allometry as in Fig. 2b. This work was funded by an European Research Council Consolidator Grant to A. Gardner (grant no. 771387).

References

1. Klein, R. G. *The Human Career* (The Univ. of Chicago Press, 2009), 3rd edn.
2. Brown, P. *et al.* A new small-bodied hominin from the Late Pleistocene of Flores, Indonesia. *Nature* **431**, 1055–1061 (2004).
3. Garvin, H. M. *et al.* Body size, brain size, and sexual dimorphism in *Homo naledi* from the Dinaledi Chamber. *J. Hum. Evol.* **111**, 119–138 (2017).
4. Humphrey, N. K. The social function of the intellect. In Bateson, P. P. G. & Hinde, R. A. (eds.) *Growing Points in Ethology*, 303–317 (Cambridge Univ. Press, 1976).
5. Clutton-Brock, T. H. & Harvey, P. H. Primates, brains and ecology. *J. Zool.* **190**, 309–323 (1980).
6. Byrne, R. & Whiten, A. (eds.) *Machiavellian Intelligence* (Oxford Univ. Press, 1988).
7. Dunbar, R. I. M. The social brain hypothesis. *Evol. Anthropol.* **6**, 178–190 (1998).
8. Henrich, J. *The Secret of our Success* (Princeton Univ. Press, 2016).
9. Dunbar, R. I. M. & Shultz, S. Why are there so many explanations for primate brain evolution? *Phil. Trans. R. Soc. B* 20160244 (2017).
10. Laland, K. N. *Darwin's Unfinished Symphony* (Princeton Univ. Press, 2017).
11. Rosati, A. G. Foraging cognition: reviving the ecological intelligence hypothesis. *Trends Cogn Sci* **21**, 691–702 (2017).
12. DeCasien, A. R., Barton, R. A. & Higham, J. P. Understanding the human brain: insights from comparative biology. *Trends Cogn. Sci.* **26**, 432–445 (2022).
13. Hooper, R., Brett, B. & Thornton, A. Problems with using comparative analyses of avian brain size to test hypotheses of cognitive evolution. *PLoS ONE* **17**, e0270771 (2022).
14. Healy, S. D. *Adaptation and the Brain* (Oxford Univ. Press, Oxford, UK, 2021).
15. Will, M., Krapp, M., Stock, J. T. & Manica, A. Different environmental variables predict body size and brain size evolution in *Homo*. *Nat. Comm.* **12**, 4116 (2021).
16. Gavrilets, S. & Vose, A. The dynamics of Machiavellian intelligence. *Proc. Natl. Acad. Sci. USA* **103**, 16823–16828 (2006).
17. dos Santos, M. & West, S. A. The coevolution of cooperation and cognition in humans. *Proc. R. Soc. B* **285**, 20180723 (2018).
18. Muthukrishna, M., Doebeli, M., Chudek, M. & Henrich, J. The cultural brain hypothesis: how culture drives brain expansion, sociality, and life history. *PLOS Comp. Biol.* **14**, e1006504 (2018).
19. González-Forero, M., Faulwasser, T. & Lehmann, L. A model for brain life history evolution. *PLOS Comp. Biol.* **13**, e1005380 (2017).
20. González-Forero, M. & Gardner, A. Inference of ecological and social drivers of human brain-size evolution. *Nature* **557**, 554–557 (2018).
21. West, G. B., Brown, J. H. & Enquist, B. J. A general model for ontogenetic growth. *Nature* **413**, 628–631 (2001).
22. Aiello, L. C. & Wheeler, P. The expensive-tissue hypothesis. *Curr. Anthropol.* **36**, 199–221 (1995).
23. Kuzawa, C. W. *et al.* Metabolic costs and evolutionary implications of human brain development. *Proc. Nat. Acad. Sci. USA* **111**, 13010–13015 (2014).
24. Schaffer, W. M. The application of optimal control theory to the general life history problem. *Am. Nat.* **121**, 418–431 (1983).
25. Sydsæter, K., Hammond, P., Seierstad, A. & Strom, A. *Further Mathematics for Economic Analysis* (Prentice Hall, 2008), 2nd edn.
26. Kamien, M. I. & Schwartz, N. L. *Dynamic Optimization* (Dover, Mineola, NY, 2012), 2nd edn.
27. Dieckmann, U., Heino, M. & Parvinen, K. The adaptive dynamics of function-valued traits. *J. Theor. Biol.* **241**, 370–389 (2006).
28. Parvinen, K., Heino, M. & Dieckmann, U. Function-valued adaptive dynamics and optimal control theory. *J. Math. Biol.* **67**, 509–533 (2013).
29. González-Forero, M. A mathematical framework for evo-devo dynamics (2022). In review at *Theor. Popul. Biol.* Preprint: `https://www.biorxiv.org/content/10.1101/2021.05.17.44`
30. Wright, T. L. & Pierson, T. C. *Living with Volcanoes* (U. S. Geological Survey Circular 1073, Denver, CO, USA, 1992).
31. González-Forero, M. How development affects evolution. *Evolution* **77**, 562–579 (2023).
32. Dekaban, A. S. & Sadowsky, D. Changes in brain weights during the span of human life: Relation of brain weights to body heights and body weights. *Ann. Neurol.* **4**, 345–356 (1978).
33. Bogin, B. *Patterns of Human Growth* (Cambridge Univ. Press, Cambridge, UK, 1988).
34. Gluckman, P. D. & Hanson, M. A. Evolution, development and timing of puberty. *Trends Endocrinol. Metab.* **17**, 7–12 (2006).
35. Leigh, S. R. Brain growth, life history, and cognition in primate and human evolution. *Am. J. Primatol.* **62**, 139–164 (2004).

36. Pontzer, H. *et al.* Daily energy expenditure through the human life course. *Science* **373**, 808–812 (2021).

37. Lande, R. Quantitative genetic analysis of multivariate evolution applied to brain: body size allometry. *Evolution* **34**, 402–416 (1979).

38. Kirkpatrick, M. & Lofsvold, D. Measuring selection and constraint in the evolution of growth. *Evolution* **46**, 954–971 (1992).

39. Bogin, B. & Smith, B. H. Evolution of the human life cycle. *Am. J. Hum. Biol.* **8**, 703–716 (1996).

40. Robson, S. L. & Wood, B. Hominin life history: reconstruction and evolution. *J. Anat.* **212**, 394–425 (2008).

41. Jones, J. H. Primates and the evolution of long, slow life histories. *Curr. Biol.* **21**, R708–R717 (2011).

42. Leigh, S. R. Evolution of human growth. *Evol. Anthropol.* **10**, 223–236 (2001).

43. Tanner, J. M., Whitehouse, R. H. & Takaishi, M. Standards from birth to maturity for height, weight, height velocity, and weight velocity: British children, 1965. *Arch. Dis. Childh.* **41**, 454–471 (1966).

44. Cameron, N. & Schell, L. M. (eds.) *Human Growth and Development* (Academic Press, London, UK, 2022), 3rd edn.

45. Gasser, T. *et al.* An analysis of the mid-growth and adolescent growth spurts of height based on acceleration. *Ann. Hum. Biol.* **12**, 129–148 (1985).

46. Hauspie, R. C. & Molinari, L. Parametric models for postnatal growth. In Hauspie, R. C., Cameron, N. & Molinari, L. (eds.) *Methods in Human Growth Research*, 205–233 (Cambridge Univ. Press, Cambridge, UK, 2004).

47. Johnson, W. Modeling growth curves for epidemiology. In Cameron, N. & Schell, L. M. (eds.) *Human Growth and Development*, chap. 13, 371–390 (Academic Press, London, UK, 2022).

48. Gasser, T. *et al.* Human height growth: correlational and multivariate structure of velocity and acceleration. *Ann. Hum. Biol.* **12**, 501–515 (1985).

49. Count, E. W. Growth patterns of the human physique: an approach to kinetic anthropometry. *Hum. Biol.* **15**, 1–32 (1943).

50. Spear, L. *The Behavioral Neuroscience of Adolescence* (W. W. Norton & Company, New York, NY, USA, 2010).

51. Tanner, J. M. The regulation of human growth. *Child Dev.* **34**, 817–847 (1963).

52. Bogin, B. Catastrophe theory model for the regulation of human growth. *Hum. Biol.* **52**, 215–227 (1980).

53. Howarth, C., Peppiatt-Wildman, C. M. & Attwell, D. The energy use associated with neural computation in the cerebellum. *J. Cereb. Blood Flow Metab.* **30**, 403–414 (2010).

54. Jerison, H. J. *Evolution of the Brain and Intelligence* (Academic Press, 1973).

55. Martin, R. D. Relative brain size and basal metabolic rate in terrestrial vertebrates. *Nature* **293**, 57–60 (1981).

56. Wilson, L. A. B. *et al.* Sex differences in allometry for phenotypic traits in mice indicate that females are not scaled males. *Nat. Comm.* **13**, 7502 (2022).

57. Smaers, J. B. *et al.* The evolution of mammalian brain size. *Sci. Adv.* **7**, eabe2101 (2021).

58. Grabowski, M., Hatala, K. G., Jungers, W. L. & Richmond, B. G. Body mass estimates of homininfossils and the evolution of human body size. *J. Hum. Evol.* **85**, 75–93 (2015).

59. Kappelman, J. The evolution of body mass and relative brain size in fossil hominids. *J. Hum. Evol.* **30**, 243–276 (1996).

60. Pilbeam, D. & Gould, S. J. Size and scaling in human evolution. *Science* **186**, 892–901 (1974).

61. Waddington, C. H. Canalization of development and the inheritance of acquired characters. *Nature* **150**, 563–565 (1942).

62. Pélabon, C. *et al.* Evolution of morphological allometry. *Ann. N. Y. Acad. Sci.* **1320**, 58–75 (2014).

63. Hansen, T. F. & Houle, D. Measuring and comparing evolvability and constraint in multivariate characters. *J. Evol. Biol.* **21**, 1201–1219 (2008).

64. Walsh, B. & Lynch, M. *Evolution and Selection of Quantitative Traits* (Oxford Univ. Press, Oxford, UK, 2018).

65. Froehle, A. W. & Churchill, S. E. Energetic competition between Neandertals and anatomically modern humans. *PaleoAnthropology* 96–116 (2009).

66. Ruff, C. B., Trinkaus, E. & Holliday, T. W. Body mass and encephalization in Pleistocene *Homo*. *Nature* **387**, 173–176 (1997).

67. Rightmire, G. P. Brain size and encephalization in early to mid-pleistocene *Homo*. *Am. J. Phys. Anthropol.* **124**, 109–123 (2004).

68. McHenry, H. M. Tempo and mode in human evolution. *Proc. Natl. Acad. Sci. USA* **91**, 6780–6786 (1994).

69. McHenry, H. M. & Coffing, K. *Australopithecus* to *Homo*: transformations in body and mind. *Annu. Rev. Anthropol.* **29**, 125–146 (2000).

70. Morrissey, M. B. Selection and evolution of causally covarying traits. *Evolution* **68**, 1748–1761 (2014).

71. Hawks, J., Hunley, K., Lee, S.-H. & Wolpoff, M. Population bottlenecks and pleistocene human evolution. *Mol. Biol. Evol.* **17**, 2–22 (2000).

72. Hamilton, W. D. The moulding of senescence by natural selection. *J. Theor. Biol.* **12**, 12–45 (1966).

73. Maynard Smith, J. *et al.* Developmental constraints and evolution. *Q. Rev. Biol.* **60**, 265–287 (1985).

74. Beldade, P., Koops, K. & Brakefield, P. M. Developmental constraints versus flexibility in morphological evolution. *Nature* **416**, 844–847 (2002).

75. Montgomery, S. H., Mundy, N. I. & Barton, R. A. Brain evolution and development: adaptation, allometry and constraint. *Proc. R. Soc. B* **283**, 20160433 (2016).

76. Gould, S. J. *The Structure of Evolutionary Theory* (Belknap Press, Cambridge, MA, USA, 2002).

77. Laland, K. N. *et al.* The extended evolutionary synthesis: its structure, assumptions and predictions. *Proc. R. Soc. B* **282**, 20151019 (2015).

78. Grabowski, M. Bigger brains led to bigger bodies?: the correlated evolution of human brain and body size. *Curr. Anthropol.* **57**, 174–185 (2016).

79. Uller, T., Moczek, A. P., Watson, R. A., Brakefield, P. M. & Laland, K. N. Developmental bias and evolution: A regulatory network perspective. *Genetics* **209**, 949–966 (2018).

80. Suárez, R. & Halley, A. C. Evolution of developmental timing as a driving force of brain diversity. *Brain Behav. Evol.* **97**, 3–7 (2022).

81. Finlay, B. L. The multiple contexts of brain scaling: phenotypic integration in brain and behavioral evolution. *Brain Behav. Evol.* **97**, 83–95 (2022).

82. Fenlon, L. R. Timing as a mechanism of development and evolution in the cerebral cortex. *Brain Behav. Evol.* **97**, 8–32 (2022).

83. Mann, A. E. Hominid and cultural origins. *Man* **7**, 379–386 (1975).

84. Rosenberg, K. R. The evolution of human infancy: why it helps to be helpless. *Ann. Rev. Anthropol.* **50**, 423–440 (2021).

85. Navarrete, A., van Schaik, C. P. & Isler, K. Energetics and the evolution of human brain size. *Nature* **480**, 91–93 (2011).

86. Cranmer, K., Brehmer, J. & Louppe, G. The frontier of simulation-based inference. *Proc. Natl. Acad. Sci. USA* **117**, 30055–30062 (2020).

87. Dieckmann, U. & Law, R. The dynamical theory of coevolution: a derivation from stochastic ecological processes. *J. Math. Biol.* **34**, 579–612 (1996).

88. Metz, J., Geritz, S., Meszéna, G., Jacobs, F. & van Heerwaarden, J. Adaptive dynamics, a geometrical study of the consequences of nearly faithful reproduction. In van Strien, S. & Lunel, S. V. (eds.) *Stochastic and spatial structures of dynamical systems*, 183–231 (Konink. Nederl. Akad. Wetensch. Verh. Afd. Natuurk. Eerste Reeks, Amsterdam, Netherlands, 1996).

89. Broekmans, F. J., Faddy, M. J., Scheffer, G. & te Velde, E. R. Antral follicle counts are related to age at natural fertility loss and age at menopause. *Menopause* **11**, 607–614 (2004).

90. Kleiber, M. *The Fire of Life* (Wiley, 1961).